

Oxidation in vitro of chromium(III) dietary supplements *mer*-[Cr(pic)₃] and *trans*(S,S)-[Cr(Cys)₂][−] by hydrogen peroxide

Emilia Nieczyporowska¹ · Ewa Kita¹  · Anna Katafias¹ · Anna Bajek² · Łukasz Kaźmierski²

Received: 12 May 2017 / Accepted: 12 July 2017 / Published online: 25 July 2017
© The Author(s) 2017. This article is an open access publication

Abstract Biological tests performed using 3T3 fibroblasts indicated low cytotoxicities for the complexes *mer*-[Cr(pic)₃] and *trans*(S,S)-[Cr(Cys)₂][−], where pic = picolinate anion and Cys = cysteine. Oxidation of these complexes by hydrogen peroxide was studied in NaOH and NaHCO₃ media. Electronic (UV–Vis) and EPR spectroscopies were used to monitor the reaction course. Hydrogen peroxide oxidizes chromium(III) to both [Cr^V(O₂)₄]^{3−} and Cr^{VI}O₄^{2−} anions in alkaline media and practically completely to CrO₄^{2−} anion in bicarbonate solution. The reactions follow consecutive biphasic or simple first-order kinetics. The first-order decay of [Cr^V(O₂)₄]^{3−} anion at pH ≈ 8 was followed by EPR spectroscopy. Based on the obtained kinetic and spectroscopic data, mechanisms for the redox transformations of these chromium(III) complexes are proposed.

Introduction

Recently, there has been growing scepticism about the use of chromium(III) pharmaceuticals, mainly due to possible health risks arising from their possible oxidation to chromium(VI) which is believed to induce cancer [1–3]. Several reports have demonstrated both extra- and intracellular oxidation of chromium(III) [4–6]. The resulting chromate(VI) anion, CrO₄^{2−}, can be transferred into cells via

membrane channels suitable for the isostructural anions SO₄^{2−} and HPO₄^{2−} and subsequently converted by cellular reductants into highly reactive chromium(V) and chromium(IV) species which can cause cellular damage, apoptotic body formation and DNA cleavage [7–13]. On the other hand, it has been suggested that chromium(IV) and chromium(V) play the major role in a recently proposed redox mechanism for the antidiabetic activity of chromium pharmaceuticals [14–17]. Studies on chromium(III) behaviour in vitro are quite rare; furthermore, its oxidation was carried out either at pH values outside the biological range [18] or using non-biological oxidants such as PbO₂ [19]. Partial H₂O₂ oxidation of chromium(III) in peptide adducts of its dietary supplements in blood serum [20] and partial intracellular chromium(III) oxidation of its nutritional supplement metabolites have been observed [6]. Recently, oxidation of chromium(III) peptides has been examined, and a new fluorescent method of chromium(III) and chromium(VI) determination in cells has been developed [19, 21].

Our tests proved that chromium(III) is not oxidized by H₂O₂ in NaClO₄ and phosphate buffer media within the 7–9 pH range, whereas oxidation does occur in blood plasma at pH 7.4. This phenomenon was the starting point of this project. The work deals with in vitro redox transformation of chromium(III) cysteine and picolinate complexes, *trans*(S,S)-[Cr(Cys)₂][−] and *mer*-[Cr(pic)₃], respectively, mediated by hydrogen peroxide which is a biogenic oxidant. The selected complexes are present on the pharmaceutical market as dietary supplements, specifically a source of synthetic biochromium [22–24]. The reaction was carried out in media mimicking biological conditions, i.e. in HCO₃[−] solution of pH ≈ 8 and also in strongly alkaline media. No literature data on kinetics of oxidation of the Cr^{III}–cysteine and Cr^{III}–picolinate

✉ Ewa Kita
ewakita@chem.umk.pl

¹ Department of Inorganic and Coordination Chemistry, Faculty of Chemistry, Nicolaus Copernicus University, Toruń, Poland

² Department of Tissue Engineering, Collegium Medicum Bydgoszcz, Nicolaus Copernicus University, Toruń, Poland

complexes by H_2O_2 have been found. The following problems have focused our attention: (1) the role of HCO_3^- medium in the overall reaction, (2) the importance of hydrolytic bond splitting resulting in partial dechelation of the ligands and (3) kinetic and mechanistic differences between reactions of the cysteine and picolinato complexes.

Experimental

Materials

Cysteine, picolinic acid and other chemicals were purchased from Sigma-Aldrich and used without further purification. $\text{Na}[\text{Cr}(\text{Cys})_2] \cdot 2\text{H}_2\text{O}$ and $[\text{Cr}(\text{pic})_3]_0 \cdot \text{H}_2\text{O}$ were prepared as described in the literature [25, 26]. Chromium was determined spectrophotometrically as CrO_4^{2-} at 372 nm ($\epsilon_{372} = 4830 \text{ M}^{-1}\text{cm}^{-1}$) after decomposition of a known amount of the complex in 0.1 M NaOH solution, followed by oxidation of chromium(III) with H_2O_2 . The theoretical chromium contents of $\text{Na}[\text{Cr}(\text{Cys})_2]$ and $[\text{Cr}(\text{pic})_3]_0$ are 14.9 and 11.9%, respectively; the found values were 14.8 and 11.8%, respectively.

Biological tests

To determine the cytotoxicity of $\text{Na}[\text{Cr}(\text{Cys})_2]$ and $[\text{Cr}(\text{pic})_3]_0$ aqueous solutions on 3T3 cells, MTT assays were performed. Based on ISO 10993-5 guidelines, $\text{Na}[\text{Cr}(\text{Cys})_2]$ and $[\text{Cr}(\text{pic})_3]_0$ aqueous solutions showed no cytotoxic activity towards 3T3 cells compared to the control group. Prior to the procedure, 3T3 cells were cultured using DMEM supplemented with 10% FBS and 1% antibiotics and grown at 37 °C, 5% CO_2 , 99% humidity. The same conditions were applied during the MTT assay, and the investigated dilutions were made using the same culture media. To maintain sterility and ensure purity, both aqueous solutions were filtered using 0.22- μm syringe filters prior to further use. Cells were cultured at 5×10^4 cells per 31.6 mm^2 of culture area for 24 h prior to the addition of 10, 5, 1, 0.1% v/v dilutions of the test solutions (4.0×10^{-3} M $\text{Na}[\text{Cr}(\text{Cys})_2]$ and 1.8×10^{-3} M $[\text{Cr}(\text{pic})_3]_0$), and the MTT assay was performed 24, 48 and 72 h after the addition of the test compound (the MTT assay was performed partially using ISO 10993-5 guidelines (Fig. 1)). Each experimental and control group contained at least eight well replications, and the entire experiment was repeated twice at different time points, yielding the same results. The investigated solutions did not exhibit cytotoxic properties compared to the control group, but cells grown using 5, 1 and 0.1% $\text{Na}[\text{Cr}(\text{Cys})_2]$ exhibited considerably higher proliferation rates at 48 and

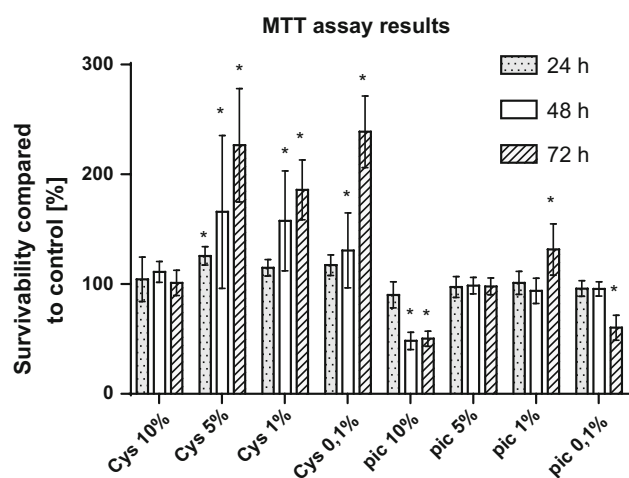


Fig. 1 Effect of $\text{Na}[\text{Cr}(\text{Cys})_2]$ (Cys) and $[\text{Cr}(\text{pic})_3]_0$ (pic) on 3T3 cells survivability after 24, 48 and 72 h of treatment. Cell cytotoxicity was determined by MTT assay and expressed as per cent of living cells compared to control group and presented as mean \pm SD, * $P < 0.05$, ANOVA-test and Dunnett's post hoc versus the control group

72 h after supplementation. Visual analysis using a phase-contrast microscope shows no morphological changes in the studied groups, except for minor morphological changes in cells cultured using 10% $\text{Na}[\text{Cr}(\text{Cys})_2]$ which might result from a high dilution factor of the base medium itself.

Kinetic measurements

The kinetic profiles of the reactions were examined spectrophotometrically using a Hewlett-Packard 8453 diode-array spectrophotometer thermostated with a HP 899090A Peltier temperature controller or using an external Julabo F25 cryostat. All experiments were performed under pseudo-first-order limiting conditions by applying an excess of hydrogen peroxide and sodium hydroxide at 298 K.

The rates of oxidation of both complexes were followed via the absorbance increase over the spectral range 340–420 nm. The reactions were initiated by injection of 0.1 cm^3 of the complex solution to 1.9 cm^3 of the thermally equilibrated medium solution, prepared in a 1 cm cell directly before the measurement, from appropriate amounts of NaOH or NaHCO_3 and H_2O_2 stock solutions. The concentration of chromium(III) complex was ca. 1.5×10^{-4} M. Kinetics of the reaction was investigated as a function of the hydrogen peroxide concentration (0.1–1.0 M) in 0.6 M NaOH (taking into account its neutralization by H_2O_2) and bicarbonate concentration (0.3–0.9 M) at 0.2 M H_2O_2 . The sodium hydroxide concentration was accurate to ca. 1% and hydrogen peroxide to ca. 5%. The ionic strength was maintained at 2.0 M (strongly alkaline media) and 1.0 M (bicarbonate solutions) with NaClO_4 . The pH of the bicarbonate

solutions was ca. 8. Additionally, some kinetic traces were recorded within the visible spectral range. The concentration of the soluble $\text{Na}[\text{Cr}(\text{Cys})_2]$ complex was ca. 1×10^{-2} M (1 cm cell). Due to the low solubility of $[\text{Cr}(\text{pic})_3]^0$, its concentration was only 1×10^{-4} M and the reaction was carried out in a 5 cm cell. Oxidation was initiated by mixing equal volumes of the thermally equilibrated complex and other component solutions.

Each kinetic run was performed for at least three half-lives of the reactions and repeated three times. Absorbance–time changes observed for the cysteine complex reaction obeyed a consecutive first-order reaction model, $\text{A} \rightarrow \text{B} \rightarrow \text{C}$. The data obtained for the $[\text{Cr}(\text{pic})_3]^0$ complex oxidation were reproduced by a simple $\text{A} \rightarrow \text{B}$ reaction model; however, at the highest $[\text{H}_2\text{O}_2]$ in NaOH solution a better fit was obtained for the consecutive reaction pattern. The results were independent of the fitting method (multifunctional analyses of the overall spectra using SPECFIT software for a $\text{A} \rightarrow \text{B} \rightarrow \text{C}$ reaction model or EnzFitter software for the two separated consecutive reaction steps). The calculated k_{obs} values were independent of the initial complex concentration.

EPR measurements

EPR spectra of reaction mixtures, composed of $\text{Na}[\text{Cr}(\text{Cys})_2]$ or $[\text{Cr}(\text{pic})_2]$ plus hydrogen peroxide in NaOH or bicarbonate solution, were recorded with a Radiopan EPR SE/X 2541 M spectrometer in X band (ca. 9.33 GHz) with a 100 kHz modulation. The microwave frequency was monitored with a frequency meter. The magnetic field was measured with an automatic NMR-type magnetometer. A flat quartz cell was used. Spectra were recorded at room temperature, and measurements started ca. 180 s after mixing of reagents of the following concentrations: $[\text{Cr}^{\text{III}}] = 1.5\text{--}1.8 \times 10^{-4}$ M, $[\text{H}_2\text{O}_2] = 0.2$ or 0.8 M, $[\text{NaOH}] = 0.6$ M or $[\text{NaHCO}_3] = 0.7$ M. The initial intensity of the EPR signal (ca. 180 s after initiation) observed for the reactions carried out in NaOH solution was relatively weak but quickly increased during the reaction course, reaching a maximum at a time dependent mainly on the system studied. For the reaction of the $[\text{Cr}(\text{Cys})_2]^-$ complex in bicarbonate– H_2O_2 solution, the initial intensity of the EPR signal (ca. 180 s after initiation) was high and then decreased during the reaction course. The collected signal intensity versus time data show a first-order decay of the chromium(V) complex. The product chromium(V) species was identified as $[\text{Cr}^{\text{V}}(\text{O}_2)_4]^{3-}$ based on its EPR parameters, which were identical with those reported in the literature [27, 28]. No EPR signal was registered for the $[\text{Cr}(\text{pic})_3]^0$ system under the same experimental conditions.

Results and discussion

A large decrease in pH from 13 to 8 results in some important thermodynamic and kinetic consequences for chromium(III)–hydrogen peroxide systems. Both the thermodynamic stability of chromium(III) and redox potential of the $\text{H}_2\text{O}_2/\text{H}_2\text{O}$ couple increase with decreasing pH. As a consequence, there is no big change in the thermodynamic driving force of the reaction within the examined pH range. However, our tests showed that the chromium(III) complexes are easily oxidized at pH 13–14 but redox stable at pH 6–8. Addition of NaHCO_3 to the system containing hydrogen peroxide and the chromium(III) complex initiates transformation of chromium(III) into CrO_4^{2-} at room temperature. This indicates that several kinetic factors are decisive for the reaction. Firstly, since the pK_a value of H_2O_2 is 11.3, hydrogen peroxide exists in two different protolytic forms in the selected pH ranges: specifically the HO_2^- anion and its conjugate acid H_2O_2 at pH 13–14 and 6–8, respectively. In the presence of HCO_3^- , peroxocarbonates are formed. Secondly, in strongly alkaline media the equilibrium between the complex with the open and closed chelate ring is shifted to the latter, which retards an inner sphere electron transfer [25, 26].

Oxidation reactions of the *mer*- $[\text{Cr}(\text{pic})_3]$ and *trans*(S,S)- $[\text{Cr}(\text{Cys})_2]^-$ complexes were monitored spectrophotometrically within the UV–Vis range and by EPR spectroscopy. Experiments were carried out in NaOH and NaHCO_3 solutions.

Strongly alkaline media

Isomer *mer*- $[\text{Cr}(\text{pic})_3]$ is slowly oxidized by H_2O_2 at 298 K. Characteristic features of this reaction are shown in Figs. 2 and 3.

An absorbance increase in the UV region (Fig. 2a) demonstrates accumulation of CrO_4^{2-} accompanied by formation of chromium(V) species, detected as an increase in the characteristic EPR signal (Fig. 3). The presence of chromium(V) is additionally confirmed by a narrow band at 740 nm (Fig. 2b) as observed in other systems [29]. The chromium(V) complex produced spectroscopically is identical to that observed in our previous studies [18, 30, 31] and has been identified as $[\text{Cr}(\text{O}_2)_4]^{3-}$. The red shift of the lower-energy d–d transition band clearly demonstrates hydrolytic transformation of the starting complex to another chromium(III) species as a result of the $\text{Cr}^{\text{III}}\text{--N}$ bond splitting and concomitant chelate ring opening. Comparison of the rate of this process with the rate of chromium(V, VI) formation shows that the latter is preceded by ligand substitution in the starting chromium(III) complex.

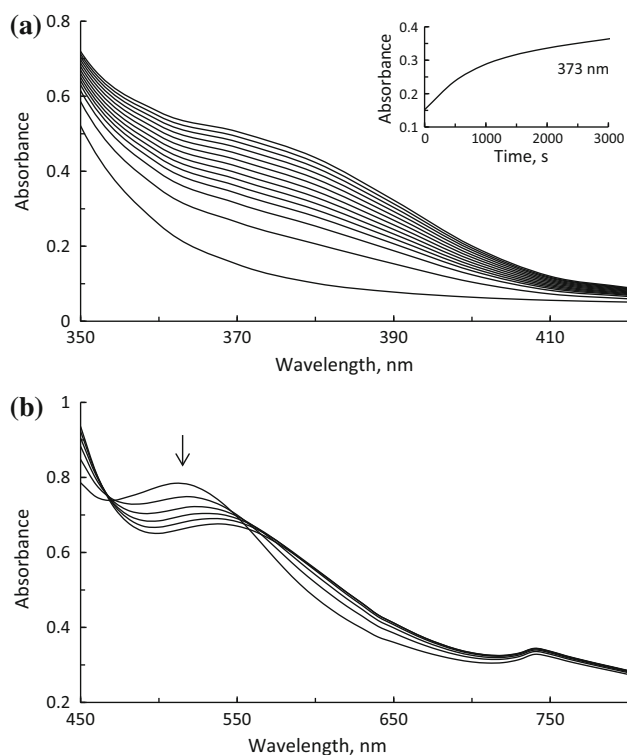


Fig. 2 Spectral changes observed during the oxidation of $[\text{Cr}(\text{pic})_3]^0$ by H_2O_2 in 0.6 M NaOH at 298 K; $[\text{Cr}^{\text{III}}] = 1.5 \times 10^{-4}$ M, $[\text{H}_2\text{O}_2] = 0.8$ M, $l = 1$ cm (a) and $[\text{Cr}^{\text{III}}] = 2.0 \times 10^{-3}$ M, $[\text{H}_2\text{O}_2] = 0.2$ M, $l = 5$ cm (b), $l = 2.0$ M, scans every 720 s

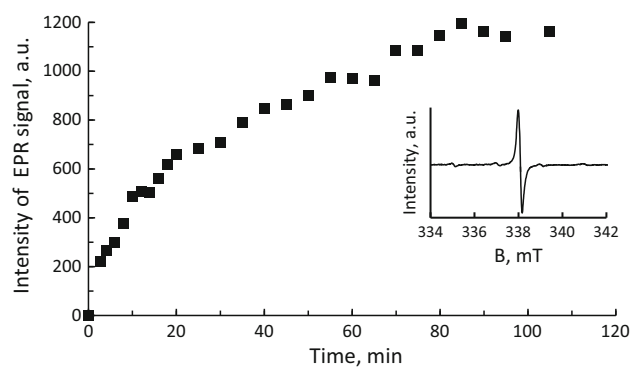


Fig. 3 Changes of the EPR signal intensity generated during oxidation of $[\text{Cr}(\text{pic})_3]^0$; $[\text{Cr}^{\text{III}}] = 1.5 \times 10^{-4}$ M, $[\text{H}_2\text{O}_2] = 0.8$ M, $[\text{NaOH}] = 0.6$ M, $l = 2.0$ M, $T = 298$ K

Kinetics of the *mer*- $[\text{Cr}(\text{pic})_3]$ oxidation have been studied applying large excesses of H_2O_2 and OH^- . In most cases the reaction rate was determined from absorption data in the UV region (CrO_4^{2-} generation). In a few experiments, rate measurements were based on changes in the visible range decay of the starting complex and also as an increase in the EPR signal intensity [chromium(V) formation]. All the methods gave close values of the pseudo-first-order rate constants for the reaction studied:

$$\begin{aligned} d[\text{CrO}_4^{2-}]/dt &\approx -d[\text{Cr}^{\text{III}}]/dt \approx d[\text{Cr}^{\text{V}}]/dt \\ &\approx k_{\text{obs1}}[\text{mer} - \text{Cr}(\text{pic})_3] \end{aligned}$$

The overall kinetic traces were reproduced very well by applying a simple $\text{A} \rightarrow \text{B}$ reaction model. The consecutive reaction model gave a better fit only at the highest H_2O_2 concentration used. The results are presented in Table 1.

The data given in Table 1 demonstrate several characteristics for the *mer*- $[\text{Cr}(\text{pic})_3]$ oxidation. First, the value of the rate constant for decay of the starting complex, at $0.26 \times 10^{-3} \text{ s}^{-1}$, is not much different than that for the CrO_4^{2-} anion formation ($0.41 \times 10^{-3} \text{ s}^{-1}$). Values of the rate constant for the picolinato chelate ring opening determined before, extrapolated to 298 K, vary between $0.7\text{--}1.0 \times 10^{-3} \text{ s}^{-1}$ at 0.2–0.9 M Na [26] and are very close to those shown in Table 1. Thus, the rates of $\text{Cr}^{\text{III}} \rightarrow \text{Cr}^{\text{V}}$ transformation and the chelate ring opening are comparable. The rate constant for the second oxidation step is ca. 80 times lower than that for the first one, and the pseudo-first-order rate constant, k_{obs1} , is linearly dependent on the hydrogen peroxide concentration (Fig. 4).

Based on the obtained results, the reaction mechanism shown in Scheme 1 is proposed.

The hydrolytic Cr^{III} -pic chelate ring opening plays a key role in the redox process of the *mer* isomer (Scheme 1). The mechanism of base hydrolysis of *mer*- $[\text{Cr}(\text{pic})_3]^0$ was presented in our previous work [26], in which subsequent entry of a water molecule (not OH^- ion) into the chromium(III) coordination sphere precedes formation of the hydroxido complexes. In the next steps mono- and dihydroxido derivatives of the starting complex, S-OH and S-(OH)_2 , are transformed into hydroperoxidochromium(III) intermediates, I-HO_2 and I-OH-HO_2 . The linear dependence of k_{obs1} on $[\text{HO}_2^-]$ suggests that the equilibrium involving formation of the intermediate species, I-HO_2 , is shifted to the left (Fig. 4). Two-electron intramolecular transfer (k_{et}) produces a labile chromium(V) complex which subsequently undergoes fast substitution of the picolinato ligands for

Table 1 Values of k_{obs} for the $[\text{Cr}(\text{pic})_3]^0$ oxidation; $[\text{OH}^-] = 0.6$ M, $T = 298$ K, $l = 2.0$ M

$[\text{HO}_2^-]$ (M)	$10^3 k_{\text{obs1}}$ (s^{-1})	
0.2	0.41 ± 0.03	$0.26 \pm 0.03^*$
0.4	0.70 ± 0.01	
0.6	0.90 ± 0.06	
0.8	1.01 ± 0.05	
$[\text{HO}_2^-]$ (M)	$10^3 k_{\text{obs1}}$ (s^{-1})**	$10^3 k_{\text{obs2}}$ (s^{-1})**
0.8	1.58 ± 0.02	0.019 ± 0.002

* Obtained from data collected in the visible range

** Obtained using $\text{A} \rightarrow \text{B} \rightarrow \text{C}$ reaction model

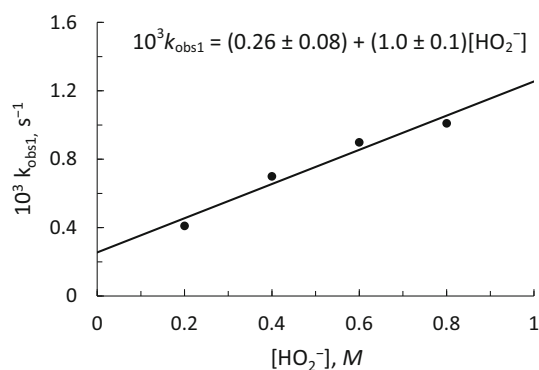
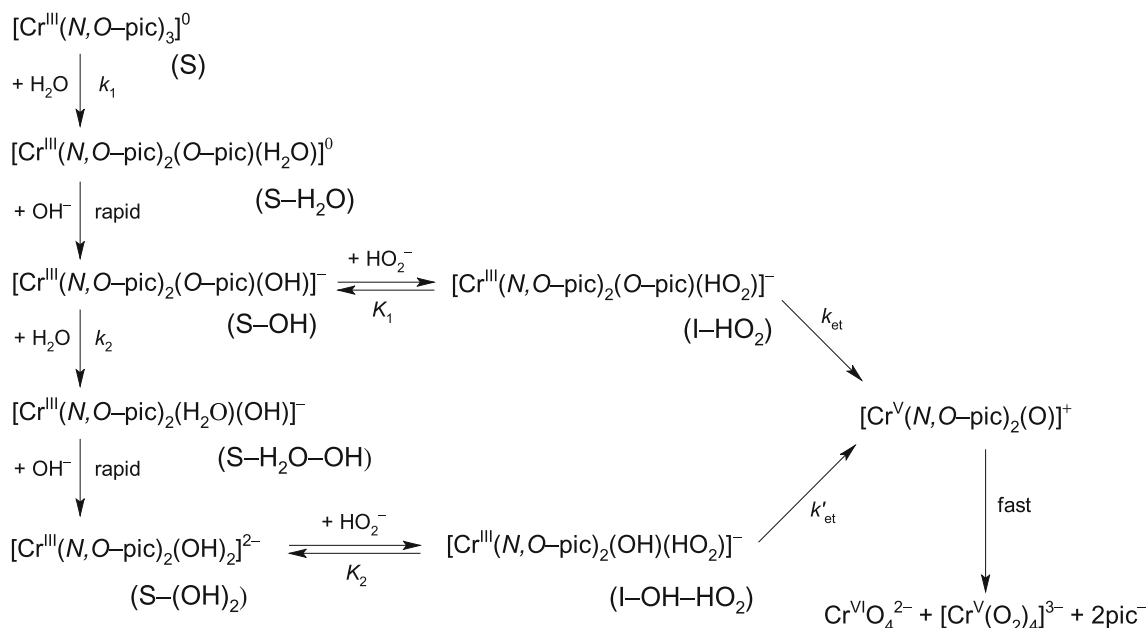


Fig. 4 Dependence of k_{obs1} on $[\text{HO}_2^-]$ for the $[\text{Cr}(\text{pic})_3]^0$ oxidation; $[\text{OH}^-] = 0.6 \text{ M}$, $T = 298 \text{ K}$, $I = 2.0 \text{ M}$

peroxido groups. Chromates(VI) are likely formed via chromium(V) disproportionation and further oxidation of chromium(IV) by hydrogen peroxide (not shown in Scheme 1). According to the proposed reaction mechanism, the slope of the plot given in Fig. 4 is interpreted as the product of the rate constant k_{et} and the equilibrium constant K_1 (formation of I-HO₂). The hydrolytic chelate ring opening is the rate-determining step of the overall redox process at the highest H₂O₂ concentration and under these conditions $k_{\text{obs1}} = k_1$. Deeper insight into the slower reaction stage is impossible due to lack of relevant data.

trans(S,S)-[Cr(Cys)₂][−]

Some notable differences between oxidation reactions of the cysteine and picolinato complexes were observed, *vide* Fig. 5.



Scheme 1 Proposed mechanism for oxidation of *mer*-[Cr(pic)₃]⁰ by hydrogen peroxide in NaOH solution

As shown in Fig. 5c, on addition of hydrogen peroxide to the $[\text{Cr}(\text{Cys})_2]^-$ alkaline solution, a practically instantaneous disappearance of the CT absorption band ($\lambda_{\text{max}} = 258 \text{ nm}$) characteristic for $\text{Cr}^{\text{III}}-\text{S}^{\text{II}}$ is followed by a substantial absorption increase at $\lambda_{\text{max}} = 372 \text{ nm}$ confirming accumulation of CrO_4^{2-} (Fig. 5a). Clearly, oxidation of the sulphur atoms precedes oxidation of chromium(III). A shift of the low energy band from 607 to 577 nm (Fig. 5b) shows transformation of the starting complex into another chromium(III) species.

Absorption changes in the visible region are very similar to those observed for base hydrolysis of the cysteine complex [25]. In the first, fast reaction stage, the low energy band shifts towards lower wavelengths and the absorbance slightly increases. The slower subsequent reaction stage is accompanied by a large absorbance decrease and a smaller blue shift. A higher ligand field strength of the generated chromium(III) complexes is consistent with Cr–S bond cleavage and introduction of OH[−] ligands to the inner coordination sphere. The rate of the subsequent $\text{Cr}^{\text{III}} \rightarrow \text{Cr}^{\text{VI}}$ oxidation is not fast enough to prevent accumulation of these chromium(III) species in the system. EPR data recorded during the reaction course demonstrated generation of $[\text{Cr}^{\text{V}}(\text{O}_2)_4]^{3-}$ in parallel with CrO_4^{2-} formation. These data are similar to those presented in Fig. 3 for the *mer*-[Cr(pic)₃]⁰ isomer. Moreover, the presence of chromium(V) is confirmed by a weak absorption band at $\lambda_{\text{max}} 740 \text{ nm}$ (Fig. 5b). A simplified reaction course is presented in Scheme 2.

In this mechanism, redox transformation of *trans*(S,S)-[Cr(Cys)₂][−] by hydrogen peroxide is initiated by rapid oxidation of the sulphur atoms and transformation of the

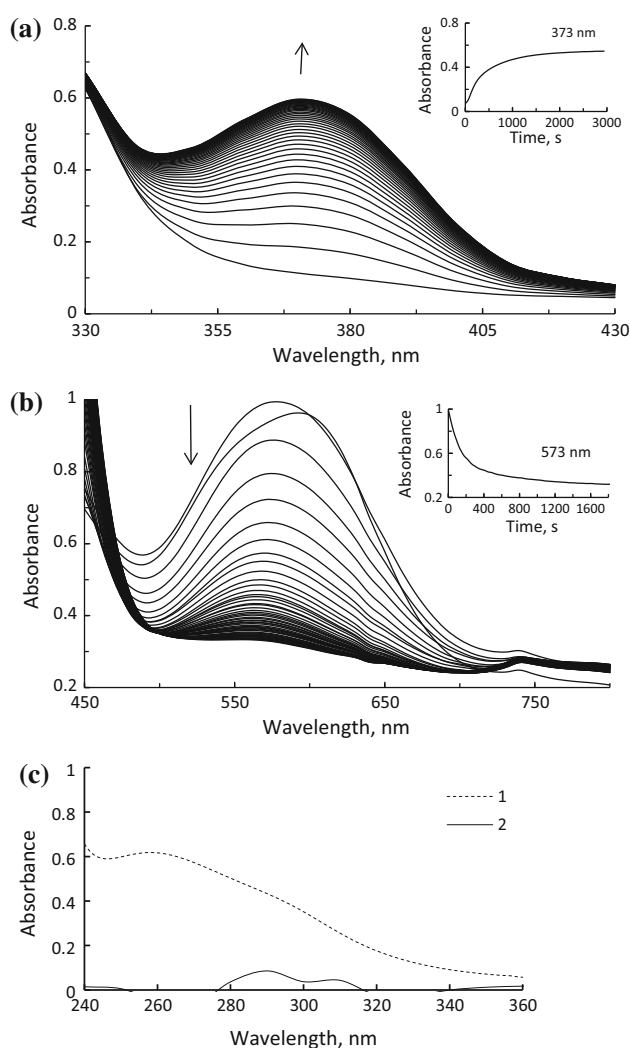
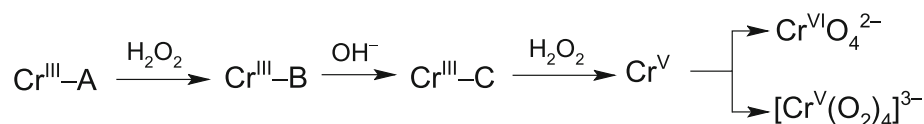


Fig. 5 Spectral changes observed during the oxidation reaction of $[\text{Cr}(\text{Cys})_2]^-$ by 0.2 M H_2O_2 in 0.6 M NaOH, $l = 1$ cm; $[\text{Cr}^{\text{III}}] = 1.6 \times 10^{-4}$ M, scans every 60 s (a); $[\text{Cr}^{\text{III}}] = 1.2 \times 10^{-2}$ M, scans every 30 s (b); $[\text{Cr}^{\text{III}}] = 5.5 \times 10^{-5}$ M, spectra 1 and 2 recorded before and immediately after addition of H_2O_2 (c)

starting complex ($\text{Cr}^{\text{III}}\text{-A}$) into a $\text{Cr}^{\text{III}}\text{-B}$ species. This reaction is much faster than the subsequent hydrolytic Cr–S bond cleavage. The $\text{Cr}^{\text{III}}\text{-B}$ intermediate (of unknown structure) is hydrolytically transformed into $\text{Cr}^{\text{III}}\text{-C}$, in which the oxidized ligand is coordinated to chromium(III) by nitrogen and oxygen atoms. Both the $\text{Cr}^{\text{III}}\text{-B}$ and $\text{Cr}^{\text{III}}\text{-C}$ species are oxidized to Cr^{V} and Cr^{VI} .

Some kinetic data for the *trans*(S,S)- $[\text{Cr}(\text{Cys})_2]^-$ isomer oxidation are shown in Fig. 5a, b. The reaction obeys two first-



Scheme 2 Oxidation of *trans*(S,S)- $[\text{Cr}(\text{Cys})_2]^-$ by hydrogen peroxide in alkaline medium

order consecutive reaction models, $\text{A} \rightarrow \text{B} \rightarrow \text{C}$. The values of the k_{obs1} and k_{obs2} for these two steps, calculated based on (1) visible spectral changes accompanying disappearance of chromium(III) and (2) UV changes accompanying formation of CrO_4^{2-} ion, are convergent to within 10–15% (k_{obs1}) or 5–7% (k_{obs2}). The results are collected in Table 2.

Comparison of the rate constants for hydrolytic Cr–S bond splitting published previously [25] with the rate constants k_{obs1} and k_{obs2} gives some insight into the reaction mechanism. The value of the rate constant at 298 K (0.6 M NaOH) for the first Cr–S bond cleavage was found to be $43 \times 10^{-3} \text{ s}^{-1}$ [25], whereas k_{obs1} increases from 4.4 to $69 \times 10^{-3} \text{ s}^{-1}$ with increasing hydrogen peroxide concentration. Thus, the rate of the oxidation process is slower than the rate of the hydrolytic chelate ring opening, with the exception of the highest oxidant concentration. The rate constants for the second Cr–S bond cleavage and the second oxidation stage are very similar at 298 K (0.6 M NaOH): $1.4 \times 10^{-3} \text{ s}^{-1}$ (hydrolytic Cr–S bond splitting) and $1.1\text{--}2.8 \times 10^{-3} \text{ s}^{-1}$ (chromium(III) oxidation). In spite of similarities between the values of the rate constants in these two systems, it should be kept in mind that in the absence of H_2O_2 , the $\text{Cr}^{\text{III}}\text{-S}^{\text{II}}$ bond cleavage takes place, whereas in the presence of H_2O_2 the $\text{Cr}^{\text{III}}\text{-S}^{\text{I}}$ bond is broken.

The dependence of k_{obs1} and k_{obs2} on $[\text{HO}_2^-]$ is described by two different functions, specifically parabolic (k_{obs1} , Fig. 6) and linear (k_{obs2} , Fig. 7).

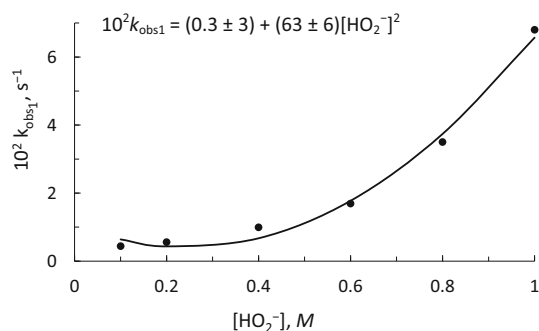
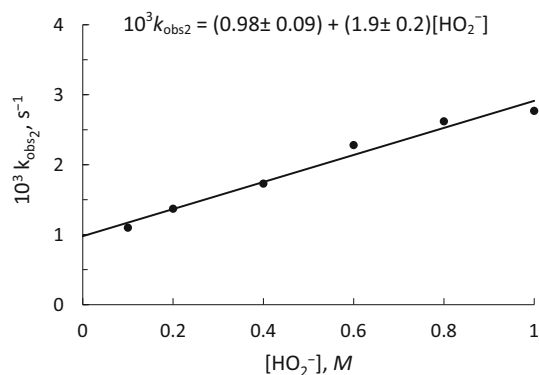
The obtained UV–Vis and EPR spectroscopic and kinetic data are consistent with the reaction mechanism presented in a simplified form in Scheme 3.

It is assumed that the *trans* isomer exists in equilibrium with its *cis* form. The two neighbouring sulphur atoms are then oxidized by hydrogen peroxide, and the $\text{S}^{\text{I}}\text{-S}^{\text{I}}$ bond is formed to give S_{ox} (where two Cys ligands are transformed into a new ligand Cys'). This oxidation stage results in a rapid disappearance of the $\text{Cr}^{\text{III}}\text{-S}^{\text{II}}$ CT band. The further oxidation steps are preceded by cleavage of the $\text{Cr}^{\text{III}}\text{-S}^{\text{I}}$ bonds, resulting in partial dechelation of the Cys' ligand and formation of the mono- and dihydroxido derivatives, $\text{S}_{\text{ox}}\text{-OH}$ and $\text{S}_{\text{ox}}\text{-(OH)}_2$. These reaction steps cause changes in the Vis spectrum, namely a blue shift of the lower energy band, characteristic of formation of a new chromium(III) complex with a higher ligand field strength. The $\text{S}_{\text{ox}}\text{-OH}$ and $\text{S}_{\text{ox}}\text{-(OH)}_2$ complexes are reversibly transformed into $\text{Cr}^{\text{III}}\text{-hydroperoxido}$ intermediates: I-HO_2 and I-OH-HO_2 (K_1 , K_2). These equilibria are shifted

Table 2 Dependence of $k_{\text{obs}1}$ and $k_{\text{obs}2}$ on $[\text{HO}_2^-]$ for oxidation of $\text{trans}(\text{S,S})\text{-}[\text{Cr}(\text{Cys})_2]^-$; $[\text{OH}^-] = 0.6 \text{ M}$, $T = 298 \text{ K}$, $I = 2.0 \text{ M}$

$[\text{HO}_2^-] \text{ (M)}$	$10^3 k_{\text{obs}1} \text{ (s}^{-1}\text{)}$	$10^3 k_{\text{obs}2} \text{ (s}^{-1}\text{)}$
0.1	4.4 ± 0.1	1.10 ± 0.02
0.2	5.6 ± 0.2	1.37 ± 0.03
	$6.4 \pm 0.2^*$	$1.26 \pm 0.03^*$
0.4	9.9 ± 0.6	1.73 ± 0.02
0.6	17 ± 1	2.28 ± 0.08
0.8	35 ± 2	2.62 ± 0.04
1.0	68 ± 3	2.77 ± 0.01

* Obtained from data collected in the visible range

**Fig. 6** Dependence of $k_{\text{obs}1}$ on $[\text{HO}_2^-]$ for the $\text{trans}(\text{S,S})\text{-}[\text{Cr}(\text{Cys})_2]^-$ oxidation**Fig. 7** Dependence of $k_{\text{obs}2}$ on $[\text{HO}_2^-]$ for the $\text{trans}(\text{S,S})\text{-}[\text{Cr}(\text{Cys})_2]^-$ oxidation

towards the hydroxo species, which is consistent with the linear $k_{\text{obs}2}$ versus $[\text{HO}_2^-]$ dependence. The $c[\text{HO}_2^-]^2$ term, in the expression describing the dependence of $k_{\text{obs}1}$ on $[\text{HO}_2^-]$, can be rationalized assuming involvement of two HO_2^- ions in the synchronic oxidation of $\text{Cr}^{\text{III}} \rightarrow \text{Cr}^{\text{V}}$ and $\text{S}^{-\text{I}} \rightarrow \text{S}^{+\text{I}}$, where one HO_2^- ion is in the inner coordination sphere and a second, free HO_2^- , interacts with the coordinated sulphur atom from bulk solution. Chromium(III) cannot be transformed into chromium(V) as long as the coordinated sulphur atom is in a negative

oxidation state. In the subsequent, faster steps cysteine is oxidized to the hydroxoacid, $\text{Cys}''(\text{OH})_2$, and sulphur to the SO_4^{2-} ion. The final products of chromium(III) oxidation are the metastable $[\text{Cr}(\text{O}_2)_4]^{3-}$ complex and CrO_4^{2-} ion, as also proposed for the $\text{mer-}[\text{Cr}(\text{pic})_3]^0$ system. Our suggestions concerning redox transformations of the cysteine ligand are based on the data given in Sharma's monograph [32] and references therein.

Formation of $\text{S}_{\text{ox}}\text{-OH}$ (k_1) and $\text{S}_{\text{ox}}\text{-(OH)}_2$ (k_2) is the rate-limiting steps for the overall redox process at H_2O_2 concentrations much higher than those applied. Under the conditions applied in this study, the rate constants of the electron transfer (k_{et} and k_{et}') and equilibrium constants (K_1 and K_2) determine the rate of chromium(V) and chromium(VI) formation. The slope of the plot in Fig. 7 is the product of the equilibrium constant K_2 and first-order rate constant k_{et}' , whilst the c parameter in the parabolic function (Fig. 6) is the product of the equilibrium constant K_1 and second-order rate constant k_{et} .

Bicarbonate media

Oxidation of chromium(III) complexes in media other than strongly alkaline ones requires the presence of HCO_3^- anions. Equilibria in the $\text{HCO}_3^- \text{-H}_2\text{O}_2 \text{-H}_2\text{O}$ system are shown in Scheme 4.

No data on the equilibrium constants describing the carbonate–hydrogen peroxide system have been found in the literature. Hence, $[\text{H}_2\text{O}_2]_t$ and $[\text{NaHCO}_3]_t$ as used in this paper denote the total concentrations of hydrogen peroxide and bicarbonates, independent of their chemical form present in the $\text{HCO}_3^- \text{-H}_2\text{O}_2 \text{-H}_2\text{O}$ system (see Scheme 4).

Formation of the final chromium(III) oxidation product, i.e. the CrO_4^{2-} anion, has been monitored from the electronic spectra in the UV region (Figs. 8, 9). The values of the A_{max} at 372 nm indicate practically complete conversion of the chromium(III) complexes into CrO_4^{2-} ion. No EPR signal was observed during the oxidation process of the $\text{mer-}[\text{Cr}(\text{pic})_3]^0$ isomer over the whole $[\text{H}_2\text{O}_2]_t$ range applied. In contrast, chromium(V) was detected at the initial stage of the $\text{trans}(\text{S,S})\text{-}[\text{Cr}(\text{Cys})_2]^-$ oxidation (Fig. 10).

The absorbance versus time data collected for the cysteine complex oxidation can be satisfactorily reproduced by a double exponential consecutive first-order $\text{A} \rightarrow \text{B} \rightarrow \text{C}$ reaction pattern (Fig. 9b), whilst for the picolinato system a good fit was obtained using a simple $\text{A} \rightarrow \text{B}$ reaction model (Fig. 9a).

$\text{mer-}[\text{Cr}(\text{pic})_3]^0$

Values of the pseudo-first-order rate constants, k_{obs} , obtained for the $\text{mer-}[\text{Cr}(\text{pic})_3]^0$ isomer oxidation are presented in Table 3.

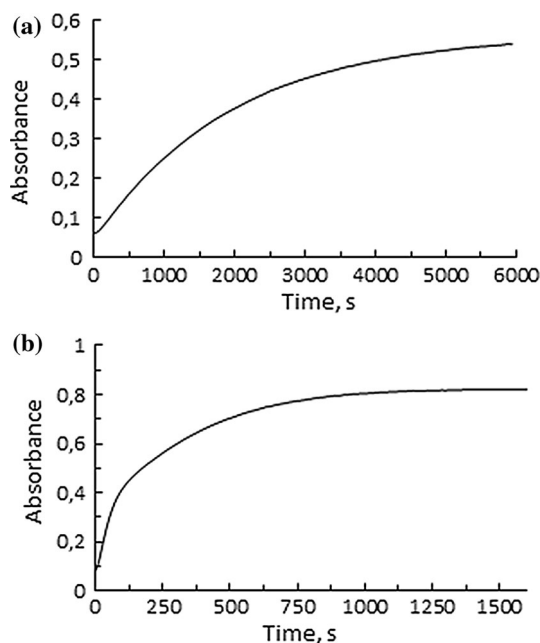


Fig. 9 Kinetic traces at 372 nm during oxidation of *mer*-[Cr(pic)₃]⁰ (a) and *trans*(S,S)-[Cr(Cys)₂]⁻ complexes (b) by H₂O₂ in bicarbonate media at 298 K; [H₂O₂]_t = 0.2 M, [HCO₃⁻]_t = 0.7 M, [Cr^{III}] = 1.2 × 10⁻⁴ M (a) and [Cr^{III}] = 1.7 × 10⁻⁴ M (b)

Oxidation of trans(S,S)-[Cr(Cys)2]⁻

An important difference between the picolinato and cysteine complexes is observed in the initial reaction phase. Oxidation of the sulphur atoms, deduced from disappearance of the CT Cr^{III}-S^{-II} bond at 258 nm, is practically instant, as was observed for the reaction in NaOH media (Fig. 5c). An unstable chromium(V) species was then detected during the oxidation process (Fig. 10). It is the same [Cr(O₂)₄]³⁻ anion as observed in NaOH media. Its concentration reaches a maximum at the very beginning of the reaction and then decreases according to a simple first-order rate law. The obtained value of the pseudo-first-order rate constant for the [Cr(O₂)₄]³⁻ decay is (6.78 ± 0.26) × 10⁻³ s⁻¹.

Oxidation of the Cr^{III}-Cys complex by H₂O₂ in NaHCO₃ media follows a biphasic A → B → C course and results in conversion of chromium(III) to CrO₄²⁻. Values of

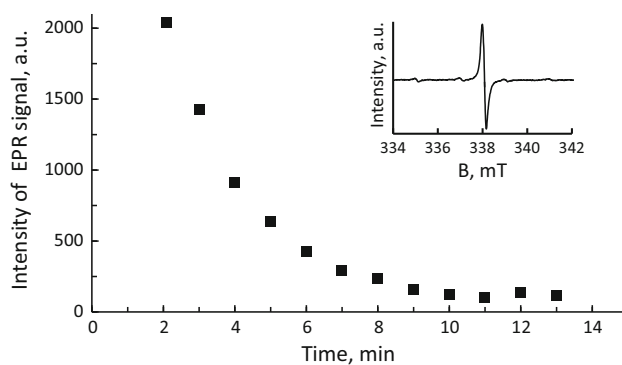


Fig. 10 Changes of the EPR signal intensity generated during oxidation of *trans*(S,S)-[Cr(Cys)₂]⁻; [Cr^{III}] = 1.8 × 10⁻⁴ M, [H₂O₂]_t = 0.2 M, [HCO₃⁻]_t = 0.7 M, I = 1.0 M, T = 298 K

Table 3 Dependence of *k*_{obs} on [HCO₃⁻]_t for the *mer*-[Cr(pic)₃]⁰ oxidation in 0.2 M H₂O₂; T = 298 K, I = 1.0 M (NaClO₄)

[NaHCO ₃] _t (M)	10 ³ <i>k</i> _{obs} (s ⁻¹)
0.3	0.27 ± 0.06
0.5	0.35 ± 0.04
0.7	0.48 ± 0.06
0.9	0.61 ± 0.04

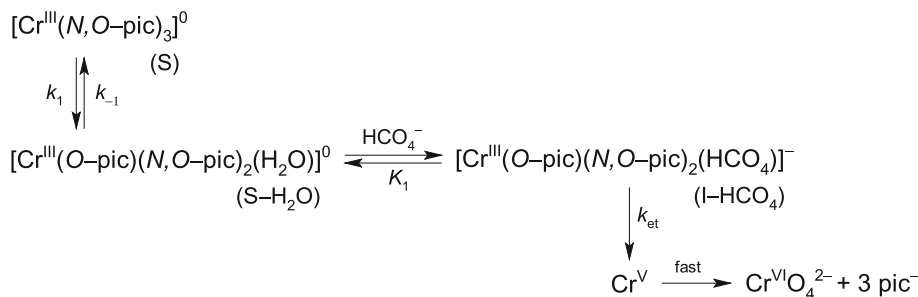
Table 4 Dependence of *k*_{obs1} and *k*_{obs2} on [HCO₃⁻]_t for the *trans*(S,S)-[Cr(Cys)₂]⁻ oxidation by 0.2 M [H₂O₂]_t, T = 298 K, I = 1.0 M (NaClO₄)

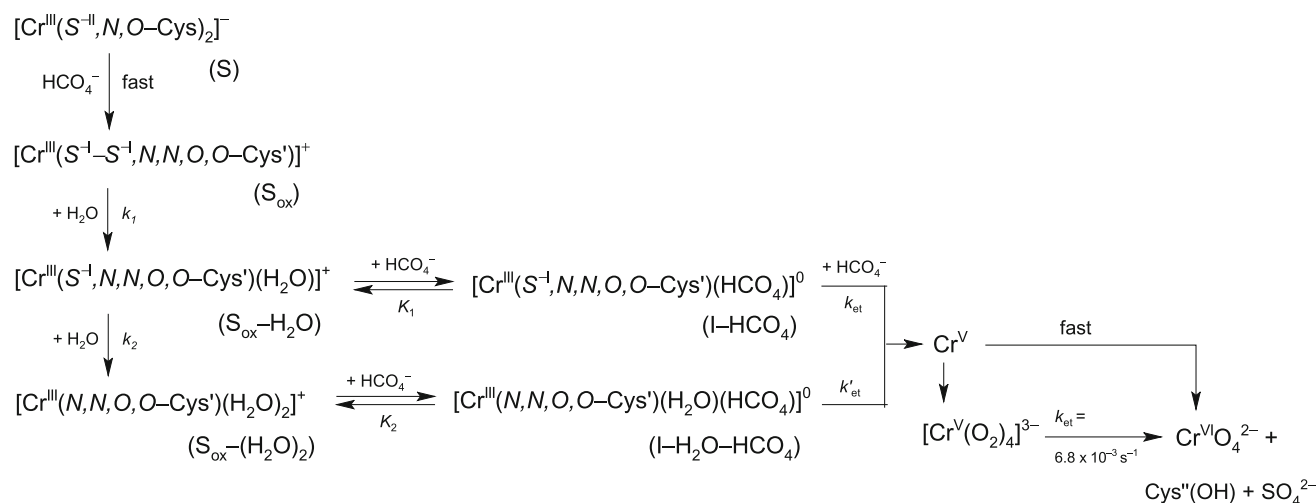
[NaHCO ₃] _t (M)	10 ³ <i>k</i> _{obs1} (s ⁻¹)	10 ³ <i>k</i> _{obs2} (s ⁻¹)
0.3	20.8 ± 0.1	2.24 ± 0.02
0.5	23.5 ± 0.4	2.31 ± 0.01
0.7	31.8 ± 0.8	2.97 ± 0.01
0.9	39 ± 1	3.40 ± 0.02

the pseudo-first-order rate constants for both of the chromium(III) oxidation stages are given in Table 4.

The data in Table 4 show that the second oxidation stage is ca. 10 times slower than the first. Moreover, an increase in bicarbonate concentration accelerates the overall process, as also observed for the *mer*-[Cr(pic)₃]⁰ system. The values of the *k*_{obs1} and *k*_{obs2} increase by about 100 and 65%, respectively, within the 0.3–0.9 M (HCO₃⁻)_t range. Rate measurements performed at 0.5 M (HCO₃⁻)_t demonstrated practically the same (within 5%) values of the rate constants within 0.2–0.8 M (H₂O₂)_t.

Scheme 5 Proposed mechanism of the *mer*-[Cr(pic)₃]⁰ oxidation by H₂O₂ in bicarbonate media





Scheme 6 Proposed mechanism of the *trans*(S,S)-[Cr(Cys)₂][−] oxidation in H₂O₂–HCO₃[−] system

The proposed reaction sequence is presented in Scheme 6.

In this mechanism, rapid oxidation of the sulphur atoms and formation of an S_{ox} precursor are followed by Cr–S bond cleavage and formation of S_{ox}–H₂O (*k*₁) and S_{ox}–(H₂O)₂ (*k*₂) chromium(III) complexes, which subsequently undergo anation by peroxocarbonate to produce I–HCO₄ (*K*₁) and I–H₂O–HCO₄ (*K*₂) intermediates. In the subsequent step, electron transfer from chromium(III) to the coordinated peroxocarbonates generates chromium(V). We assume that oxidation of I–HCO₄ requires the participation of an additional HCO₄[−] ion to prevent the reverse Cr^V → Cr^{III} reduction by coordinated sulphur in a negative oxidation state. The next step of the process is Cr^V → Cr^{VI} transformation, for which two reaction paths are observed. The main path involves rapid decay of chromium(V) not stabilized by peroxido ligands. The minor reaction path proceeds via the rather inert [Cr^V(O₂)₄]^{3−} anion (6.8 × 10^{−3} s^{−3} at 298 K). This rate constant is ca. twice higher than the rate constant for the second oxidation stage (*k*_{obs2}). Decay of the [Cr^V(O₂)₄]^{3−} anion according to a first-order rate expression implies its intramolecular decomposition. The alternative decay mechanism, i.e. disproportionation, would require a second-order dependence.

Comparison of the rate constants given in Tables 3 and 4 clearly demonstrates a much higher redox stability of the picolinato than the cysteine complex.

Conclusions

Fundamental biological criteria, i.e. low cytotoxicity of the *mer*-[Cr(pic)₃]⁰ and *trans*(S,S)-[Cr(Cys)₂][−] complexes, qualify them as sources of synthetic biochromium.

Moreover, the fast hydrolytic Cr–S bond cleavage observed for the cysteine complex generates a chemically and biologically active site in the inner coordination sphere, making possible its interaction with biological targets. However, both of these food supplements are quite rapidly oxidized by hydrogen peroxide, giving CrO₄^{2−} ion in bicarbonate media, thus producing mutagenic and carcinogenic species of chromium in higher oxidation states. Chromium(V) present in bicarbonate media decays with a rate comparable to that of the overall redox process, but its concentration is much lower than that of CrO₄^{2−} during the overall reaction course. The picolinato complex is much more redox resistant than the cysteine one. Oxidation of the chromium(III) centre by hydrogen peroxide proceeds via an inner sphere electron transfer pathway controlled by hydrolytic chelate ring opening.

Acknowledgements E.N. would like to express her gratitude to National Science Centre for financial support of this project, grant No. 2015/17/N/ST4/04070. Authors would like to express their gratitude to prof. Grzegorz Wrzeszcz for EPR measurements.

Open Access This article is distributed under the terms of the Creative Commons Attribution 4.0 International License (<http://creativecommons.org/licenses/by/4.0/>), which permits unrestricted use, distribution, and reproduction in any medium, provided you give appropriate credit to the original author(s) and the source, provide a link to the Creative Commons license, and indicate if changes were made.

References

- Dillon CT, Lay PA, Bonin AM, Dixon NE, Collins TJ, Kostka KL (1993) Carcinogenesis 14:1875
- Bartholomäus R, Irwin JA, Shi L, Smith SM, Levina A, Lay PA (2013) Inorg Chem 52:4282
- Lay PA, Levina A (2013) In: Reedijk J, Poepelmeier K (eds) Comprehensive inorganic chemistry II. Metal carcinogens, vol 3.2, 2nd edn. Elsevier, Amsterdam, pp 835–856

4. Levina A, Lay PA (2008) *Chem Res Toxicol* 21:563
5. Levina A, Mulyani A, Lay PA (2007) In: Vincent JB (ed) *The nutritional biochemistry of chromium(III). Redox chemistry and biological activities of chromium(III) complexes*. Elsevier, Amsterdam, pp 225–256
6. Wu LE, Levina A, Harris HH, Cai Z, Lai B, Vogt S, James DE, Lay PA (2016) *Angew Chem Int Ed* 55:1742
7. Chiu A, Shi XI, Lee WKP, Hill R, Wakeman TP, Katz A, Xu B, Dalal NS, Robertson JD, Chen C, Chiu N, Donehower L (2010) *J Environ Sci Health, Part C* 3:188
8. Vincent JB (2010) *Dalton Trans* 39:3787
9. Marin R, Ahuja Y, Bose RN (2010) *J Am Chem Soc* 132:10617
10. Myers JM, Antholine WE, Myers CR (2011) *Toxicology* 281:37
11. Asatiani N, Abuladze M, Kartvelishvili T, Kulikova N, Asanishvili L, Holman H, Sapojikova N (2010) *Biometals* 23:161
12. Wise SS, Holmes AL, Qin Q, Xie H, Katsifis SP, Douglas Thompson W, Wise JP (2010) *Chem Res Toxicol* 23:365
13. Vincent JB (2007) *The nutritional biochemistry of chromium(III)*. Elsevier, Amsterdam, p 207
14. Wang ZQ, Cefalu WT (2010) *Curr Diabetes Rep* 10:145
15. Cefalu WT et al (2010) *Metab Clin Exp* 59:755
16. Abdul-Ghani MA, DeFronzo RA (2008) *Oxidative stress in aging*. Springer, Berlin, p 191
17. Ceriello A, Testa R (2009) *Diabetes Care* 32:232
18. Kiersikowska E, Kita E, Kita P, Wrzeszcz G (2016) *Transit Met Chem* 41:435
19. Headlam HA, Lay PA (2016) *J Inorg Biochem* 162:227
20. Nguyen A, Mulyani, Levina A, Lay PA (2008) *Inorg Chem* 47:4299
21. Hu X, Chai J, Liu Y, Liu B, Yang B (2016) *Spectrochim Acta Part A* 153:505
22. Trent LK, Theiding-Cancel D (1995) *J Sports Med Phys Fit* 35:273
23. Yeh GY, Eisenberg DM, Kaptchuk TJ, Philips RS (2003) *Diabetes Care* 26(4):1277
24. Slesinski RS, Clarke JJ, San RHC, Gudi R (2005) *Mutat Res* 585:86
25. Kiersikowska E, Kita E, Kita P (2015) *Transition Met Chem* 40:427
26. Marai H, Kita E, Wiśniewska J (2012) *Transit Met Chem* 37:55
27. Dalal NS, Millar JM, Jagadeesh MS, Seehra MS (1981) *J Chem Phys* 74:1916
28. Zhang L, Lay PA (1998) *Inorg Chem* 37:1729
29. Katafias A, Impert O, Kita P, Wrzeszcz G (2004) *Transit Met Chem* 29:855
30. Kiersikowska E, Marai H, Wrzeszcz G, Kita E (2013) *Transit Met Chem* 38:603
31. Kiersikowska E, Marai H, Mątewska M, Wrzeszcz G, Kita E (2014) *Transit Met Chem* 39:361
32. Sharma VK (2013) *Oxidation of amino acids, peptides, and proteins. Kinetics and mechanism*. Wiley, Hoboken